Remote sensing for glacial lakes detection: a multi-sensor approach for mapping and monitoring lakes in Western Alps

Martina Lodigiani[1], Fatima Karbou[2], Jean-Baptiste Doridant[3], Bruno Demolis[4], Maddalena Nicora[1], Guillaume James[5], Pour Adrien[6] Vivian Bonnetain[3], Saskia Gindraux[7], Luca Mondardini[1,8], Paolo Perret[1,9], Fabrizio Troilo[1]

[1] Fondazione Montagna Sicura – Montagne Sûre, Loc. Villard de La Palud 1, 11013, Courmayeur, Italy;
[2] CNRS, CNRM, Centre d'Études de la Neige, Université Grenoble Alpes, Université de Toulouse, Météo-France, Grenoble, France;
[3] ONF, Pôle Recherche Développement Innovation, Villers-lès-Nancy, France;
[4] ONF, service de Restauration des Terrains de Montagne, Grenoble, France;
[5] CNRS, Inria, Grenoble INP (Institute of Engineering Université Grenoble Alpes), LJK, Université Grenoble Alpes, Grenoble, France;
[6] Météo-France, DirOp, CMS, Lannion, France; [7] Centre de recherche sur l'environnement alpin, rue de l'Industrie 45, CH-1950 Sion;
[8] Dept. of Computer Science "Giovanni degli Antoni", University of Milano, Via Celoria 18, 20133 Milano, Italy;
[9] Dept. of Electrical, Computer Science and Biomedical Engineering, University of Pavia, Via Ferrata 1, 27100 Pavia, Italy.

Keywords: Earth Observation, Glacial Lakes, Multispectral, SAR, Copernicus.

Abstract

Glacial lakes are critical indicators of the effects climate change and significant sources of natural hazards, such as Glacial Lake Outburst Floods (GLOFs), cascading events, etc. Monitoring their formation and evolution is essential for understanding cryospheric dynamics and supporting risk management, yet systematic mapping is hindered by the complexity of high-mountain environments. Developing robust, automated methods using remote sensing remains challenging due to rugged topography, snow, ice, and shadows causing misclassification.

This paper proposes a multi-sensor methodology for glacial lake detection and monitoring, integrating optical data from Sentinel-2 and Synthetic Aperture Radar (SAR) data from Sentinel-1. The study focuses on the Western Alps using data from 2022 to 2024. The methodology applies optical indices using a double thresholding strategies and tests machine learning algorithms. On the other hand, it investigates the potential of the recently developed OASIS index for SAR-based detection, aiming to overcome cloud cover and illumination limitations inherent in optical imagery.

Preliminary results show that optical indices perform well but require dynamic thresholding, as snowmelt and shadows remain major sources of uncertainty. Machine learning approaches demonstrate good potential in mitigating these limitations. The OASIS index (SAR) proves to be a promising complementary tool, especially under cloudy conditions, though still challenged by surface roughness. The integration of optical and radar data significantly increases the robustness of lake detection and reduces temporal gaps in monitoring. This methodology contributes to advancing automated systems for hazard assessment and climate change effects monitoring in alpine regions.

1. Introduction

High-mountain environments are currently undergoing rapid and profound transformations due to global climate change. One of the most visible consequences of rising temperatures is the rapid retreat of glaciers, a phenomenon that has intensified significantly in recent decades (Zemp et al., 2025). This cryospheric downwasting is frequently accompanied by the formation of new glacial lakes or the expansion of existing ones, as meltwater accumulates in overdeepened basins or behind morainic or ice dams (Shugar et al., 2020). Although these water bodies represent potential resources for hydroelectric power and freshwater storage, they simultaneously pose significant risks to downstream communities and infrastructure (Emmer et al., 2022, Taylor et al., 2023). Interestingly, recent global assessments indicate that while the total area of glacial lakes is expanding (Zhang et al., 2024), the magnitude of individual outburst floods has shown a decreasing trend; nonetheless, the increased surface area provides a larger target for external triggers, maintaining a high level of hazard potential (Veh et al., 2025). The most critical hazard associated with these environments is the occurrence of Glacial Lake Outburst Floods (GLOFs), which can be triggered by dam failures, ice avalanches, sub-glacial drainage or landslides into the lake (Costa and Schuster, 1988). Consequently, continuous monitoring of glacial lake evolution is not only fundamental for understanding the changing dynamics of the cryosphere, but is also needed for the assessment of hazards and the reduction of disaster risk in alpine valleys.

Despite the urgency of this task, systematic mapping and monitoring of glacial lakes present substantial challenges. Traditional field-based surveys are often impractical due to the remoteness of these areas, the harsh climatic conditions, and the logistic difficulties of accessing high altitude terrain with instrumentation (Kääb et al., 2005). In this context, satellite remote sensing has emerged as the primary tool for observing high-altitude water bodies, offering the ability to acquire multi-temporal data over large areas (Nagai et al., 2017, Zheng et al., 2021).

The current state-of-the-art in glacial lake mapping is heavily based on optical satellite imagery, particularly from missions such as Landsat and Sentinel-2. Common methodologies em-

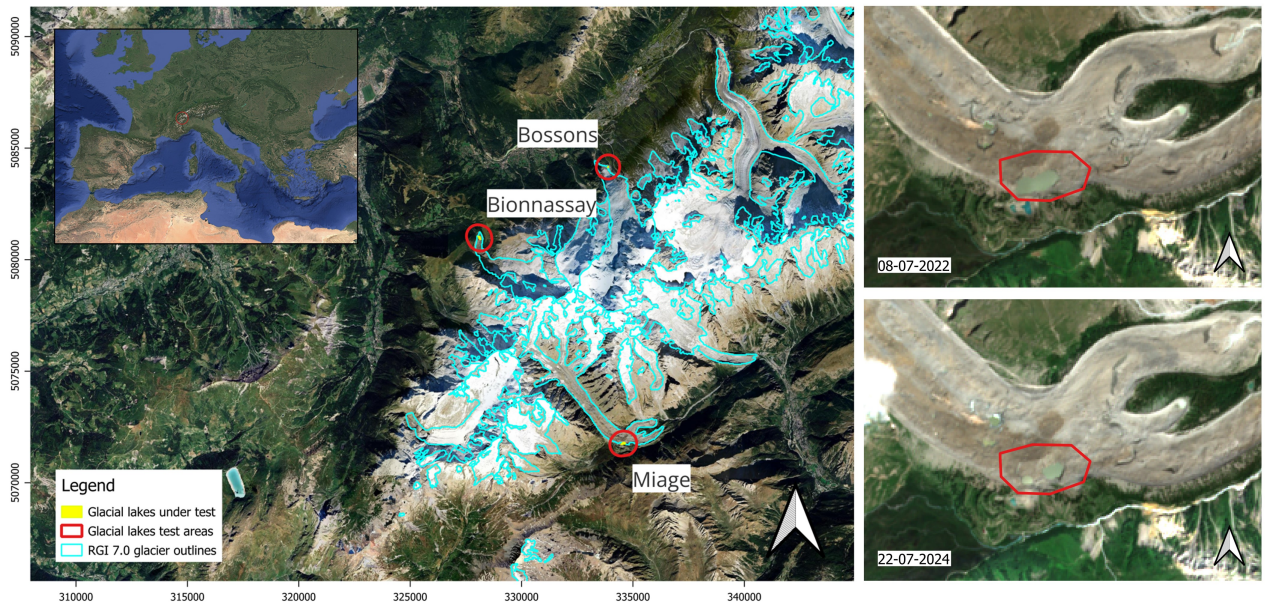

Figure 1. On the left, a satellite map of the Mont Blanc massif, where the glacier perimeters as in the RGI 7.0 inventory are outlined in light blue and most observed glacial lakes, in yellow, are buffered in red. On the right, the lake under test on the Miage glacier, in 2022 (top), when it was completely full, and in 2024 (bottom), when it was split in two smaller water basins.

ploy spectral water indices, such as the Normalized Difference Water Index (NDWI) and the Modified Normalized Difference Water Index (MNDWI), often combined with thresholding techniques to separate water from non-water pixels (Troilo et al., 2025, Bolch et al., 2008, Huggel et al., 2002). However, while optical remote sensing provides high spatial resolution and interpretability, it suffers from intrinsic limitations. High-mountain environments are characterized by frequent cloud cover, which causes significant temporal gaps in monitoring series. Furthermore, the complex spectral signature of these landscapes, where water must be distinguished from dark topographic shadows, wet snow, and glacier ice, often leads to misclassification and false positives when using standard optical indices.

Synthetic Aperture Radar (SAR) offers a theoretical solution to the limitations of optical sensors, as it can acquire data regardless of cloud cover or solar illumination. However, the use of SAR for glacial lake detection has historically been less common than optical methods due to challenges related to geometric distortions (layover and shadow) in steep terrain and the difficulty in distinguishing calm water from smooth surfaces like wet snow or sand (Wangchuk et al., 2019, Miles et al., 2017). Consequently, a robust, automated, and all-weather monitoring system that effectively mitigates the specific noise of alpine environments remains a significant knowledge gap.

To address these challenges, this study proposes and validates a multi-sensor methodology that integrates Sentinel-2 optical imagery with Sentinel-1 SAR data. The primary goal of this work is to overcome the limitations of single-sensor approaches by exploiting their complementarity. Specifically, we aim to: (i) evaluate the performance of a double thresholding and machine learning algorithms on optical indices to handle variable acquisition conditions; (ii) investigate the potential of the recently developed OASIS index for SAR-based detection in rugged terrain; and (iii) explore the possibility of combining optical and SAR workflow, together with a ML approach, in the complex topography of the Western Alps.

The remainder of this paper is organized as follows. Section 2 describes the study area in the Western Alps and the dataset employed. Section 3 details the methodological framework, including pre-processing, the calculation of optical and radar indices, and the segmentation strategies. Section 4 presents the lake detection results and validates them against reference inventories. Section 5 discusses the advantages and limitations of the proposed approach, analyzing the sources of error and the benefits of sensor integration. Finally, Section 6 draws the conclusions and outlines future research directions.

2. Study Area

The study focuses on the Western Alps, in a transfrontalier context that includes Italy and France. This region is characterized by rugged topography, with steep slopes and high-altitude glacial basins, making it a representative environment for testing remote sensing applications.

The Western Alps were selected as the primary area of interest because of their sensitivity to climate change. The region hosts a significant number of glaciers that have experienced an accelerated retreat over the last decades (Zemp et al., 2019, Huss et al., 2017). This has led to a gain of proglacial and supraglacial lakes, which often form in rock basins exposed by the retreat of the ice. It may appear that those lakes are dammed by a moraine or by an ice dam, making the presence of water unstable. The high density of these water bodies, combined with the proximity of populated valleys and infrastructure, makes this area a critical hotspot for monitoring potential Glacial Lake Outburst Flood (GLOF) hazards.

Within this broader region, a specific focus is given to test sites located in the Aosta Valley (Italy) and in the French Alps. These sub-regions were selected as key validation sites due to the availability of extensive in-situ measurements and historical records of lake evolution, which provide essential ground truth for calibrating the detection algorithms. In particular, the selected sites in the Mont Blanc area are shown in Fig. 1. Other sites in the French and Italian Alps were analyzed. However, those are not displayed for simplicity. Among the three lakes in the picture,

the Miage glacial lake was selected for this study as a primary focus site. Located on the Italian side of the Mont Blanc massif (Val Veny) at the terminus of the Miage Glacier, it represents an iconic example of a glacier-contact lake situated on a debris-covered glacier. The lake lies at an elevation of approximately 2,020 m a.s.l. and is characterized by an highly variable morphology. It is bounded by steep ice cliffs and extensive supraglacial debris, and its surface area fluctuates significantly during the melt season and through the years. Depending on the water level, the lake often separates into multiple interconnected basins separated by debris bridges.
From a remote sensing perspective, the Miage Lake poses significant challenges that make it an ideal test site for detection algorithms. The water is often highly turbid due to suspended glacial flour, reducing the spectral contrast with the surrounding gray debris in optical imagery. Furthermore, the presence of vertical ice cliffs and the rugged topography of the moraines induce severe geometric distortions in SAR data. Consequently, this site provides a critical benchmark for evaluating the robustness of the proposed multi-sensor methodology against complex environmental noise.

3. Data Analysis and Methodology

The methodology proposed in this study is based on a multi-sensor approach designed to exploit the complementarity between optical and radar observations. The primary goal is to establish a robust workflow for the automated detection of glacial lakes, minimizing the impact of environmental noise typical of alpine regions, such as topographic shadows, melting snow, and high water turbidity.

3.1 Optical data analysis

The optical workflow utilizes Sentinel-2 Level-2A Bottom-Of-Atmosphere (BOA) imagery, focusing on the summer months (June to September) to minimize snow interference and ensure maximum lake visibility. The processing chain integrates cloud and cloud shadows masking, spectral index calculation, and a multi-criteria classification logic. To ensure data quality, a local cloud-filtering strategy is applied. Rather than relying on global tile metadata, the Scene Classification Layer (SCL) is used to assess cloud and shadow presence specifically within a buffer area surrounding each target lake. Images exceeding a 20% local cloud cover are discarded, ensuring that the spectral analysis is performed only on reliable pixels.
Water bodies are identified through the calculation of the NDWI:

$$NDWI_g = \frac{\rho_{Green} - \rho_{NIR}}{\rho_{Green} + \rho_{NIR}}$$

where ρ represents the reflectance in the Green ($B3$) and NIR ($B8$) bands.
To account for the complex spectral conditions of proglacial lakes, often characterized by high turbidity due to suspended glacial flour, a dual-thresholding strategy is implemented. This approach moves beyond a single-value classification by distinguishing between a high-confidence water core and its marginal transitional zones. Specifically, a hard threshold (HT) is applied to identify certain water pixels with high spectral contrast, effectively serving as a high-probability seed for lake detection. To capture the full extent of the water body, a more sensitive soft threshold (ST) is applied. The ST is designed to include marginal cases that the more conservative HT might miss, such as shallow waters, pixels affected by high turbidity, or mixed pixels at the shoreline where the spectral signature is influenced by the surrounding debris. In Fig. 2 an example of the output obtained applying the HT ad the ST is shown for two different dates and lake conditions.

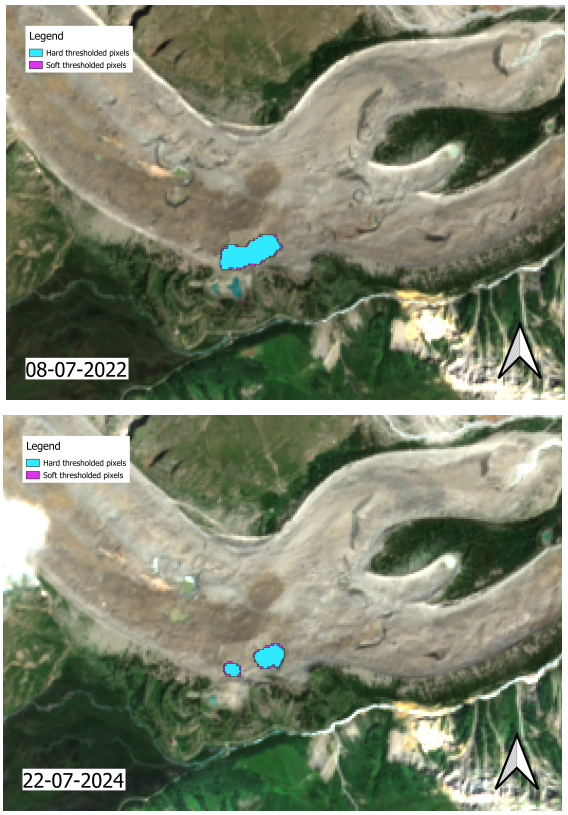

Figure 2. Automated dual-threshold segmentation results on Miage Lake using Sentinel-2 for (top) 8 July 2022 and (bottom) 22 July 2024. Blue overlays represent high-confidence water pixels identified imposing the hard threshold, while magenta pixels indicate the marginal or turbid areas captured wit the soft threshold.

A key refinement of this strategy is the application of a spatial connectivity constraint: a pixel identified using the ST is only considered valid if it belongs to a cluster that contains at least one pixel segmented by the HT. This logic ensures that the potential lake extent captured by the ST algorithm is always anchored to a high-confidence core, allowing for the rejection of isolated "soft" pixels that likely represent background noise, damp debris, or minor ephemeral ponds.
To further ensure the reliability of the output and minimize false positives, the classification is integrated with several spectral and topographic filters. Topographic shadows, which can be spectrally similar to water, are masked by excluding pixels with very low reflectance in the Blue band ($B2 < 0.03$), while a snow and ice filter is applied by masking pixels with high reflectance in the NIR band ($B8 > 0.15$) to prevent misclassification during the snowmelt season. Finally, the detection is constrained by a topographic slope filter derived from the SRTM DEM (acquired in 2000). While glacial lakes typically form in flat or gently sloping basins, the rapid geomorphological evolution of these high-mountain environments poses a significant challenge for static topographic data. Global models like the SRTM may not fully reflect recent changes, such as the transition from ice-covered slopes to exposed rock basins or new depressions. To

account for these potential inaccuracies of the DEM, a relatively broad slope limit of 30° was adopted. This threshold is wide enough to ensure that all potential water-collecting depressions are included—even where the underlying topography has evolved significantly since the DEM acquisition—while effectively ignoring steep, dark rock faces or shaded couloirs that might otherwise mimic the spectral behavior of water.

3.2 Machine learning algorithm

Complementary to the rule-based thresholding, a Machine Learning (ML) approach was implemented to provide a statistically robust classification over a broader temporal scale.

The optical data used for the ML workflow consists of Sentinel-2 Level-2A Bottom-of-Atmosphere (BOA) products. This dataset comprises 13 spectral bands with varying spatial resolutions (10 m, 20 m, and 60 m) and a 5-day temporal resolution. For this study, the time series for tile T32TLR (centered at 45.5°N, 7.1°E) was retrieved from the GEODES platform (`https://geodes.cnes.fr/projects/sentinel-2/`), maintained by the French National Centre for Space Studies (CNES). This platform provides products already corrected for atmospheric effects and includes pre-calculated masks for clouds, saturated pixels, and no-data areas. All available images from 2022 to 2024 with a local cloud cover threshold below 40% were selected, utilizing the GEODES masks for filtering. The analysis incorporated bands B2, B3, B4, B5, B6, B7, B8, B8A, B11, and B12. To standardize the input, all bands were resampled to a 10-meter spatial resolution. For each pixel, spectral values were averaged over a fifteen-day window to generate a mean temporal series. Missing values resulting from cloud or shadow interference were filled using linear interpolation (`https://www.rdocumentation.org/packages/terra/versions/1.8-86/topics/approximate`). Subsequently, three spectral indices were calculated from these averaged values:

- NDWI_g with green band, as described in Sec. 3.1;
- NDWI_b using the blue band:

$$NDWI_b = \frac{\rho_{Blue} - \rho_{NIR}}{\rho_{Blue} + \rho_{NIR}}$$

- MNDWI:

$$MNDWI = \frac{\rho_{Green} - \rho_{SWIR_1}}{\rho_{Green} + \rho_{SWIR_1}}$$

A two-class Random Forest classification algorithm (Breiman, 2001) was implemented to distinguish pixels that are IN (coded as a "1" value) or OUT (coded as a "0" value) of lakes. For the training set, a ground-based observations collected by the French National Institute of Research for Agriculture and the Environment (INRAE) was used. These observations were composed of a designation of the outlines of mountain lakes obtained by photointerpretation on images at a resolution of 20 cm taken in 2022. Only lakes within 500 meters of a glacier were selected, representing 208 lakes in the selected study area. Ground truth pixels identified as IN lakes were extracted in the area of lakes minored with a fifteen meters buffer zone. Pixels identified as OUT of lakes were selected within a fringe between 50 m and 150 m from the shores of the selected lakes. The algorithm was computed three times on a 80% random sub-sample of the training dataset, equilibrate in terms of pixels IN and OUT lakes.

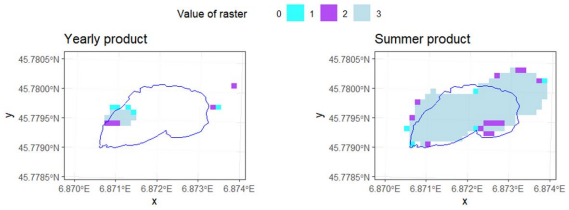

Figure 3. Comparison of the yearly product and the summer product on the lake Miage, for 2022. We can see the much better detection of the lake in comparison with the outlines of the 2022 inventory (blue line).

The final cartography was obtained by adding the three products together: the final map has values ranging from 0 (never detected as IN a lake) to 3 (detected as IN a lake by the three computations). Finally, this process was tested with different time period over which to consider spectral images: by selecting either images from the summer months (June to September, referred to as the summer product) or images from all seasons (referred to as the yearly product).
We assessed performance on the final raster using an independent validation database comprising 199 lakes obtained from the French National Geographic Institute (IGN). First, we calculated the percentage of effective lake detection on this validation database to assess the detection rate of the method: a lake was considered detected if more than one pixel within its outline was classified as IN. We then explored the proportion of over-detection by qualifying the effective detection of water areas in pixels IN using Google Maps satellite imagery as ground truth, which is available via the QuickMapsService plugin in QGIS (`https://plugins.qgis.org/plugins/quick_map_services/`). This proportion was assessed through the visual qualification of a subsample of IN pixels ($\sim$ 5% for the study area). The data were also photo-interpreted on Miage Lake to assess the IN surface area detected in the rasters obtained from different periods (summer product and yearly product).

3.3 Radar data analysis

The SAR workflow uses Sentinel-1 images with the S1Tiling tool developed by CNES and CESBIO ((Koleck and Hermitte, 2020), `https://www.github.com/CNES/S1Tiling`). The database targets the period from June to September to minimize interference due to wet snow and guarantee the best view of the lakes. The SAR images are from four Sentinel-1 orbits (two ascending, relative orbit numbers 161 and 88, and two descending, relative orbit numbers 139 and 66). The processing chain includes standard preprocessing on Sentinel-1 Level-1 GRD (Ground Range Detected), from the Interferometric Wide Swath (IW) mode, data as well as the calculation of the so called oasis index (Karbou et al., 2026), a highly sensitive index to water, from two ascending and descending orbit images taken 36 hours apart. We end up with 20 meter resolution time series of calibrated and orthorectified Sentinel-1 backscatter images and derived oasis index images from 2022 to 2024. The oasis index is formulated to give high values when both orbits observe the same area with low backscatter, which is the case with lakes. If only one orbit observes a region of low backscatter, possibly due to shadow zones, the oasis index values will be close to zero. The index amplifies signals from regions exhibiting specular or near-specular behavior. As an example, the SAR backscatter in VV polarisation from the descending orbit D139 on July 5, 2022, and the ascending orbit A161 on July 6, 2022, are shown in Fig. 4 (top panels). The corresponding oasis index map is

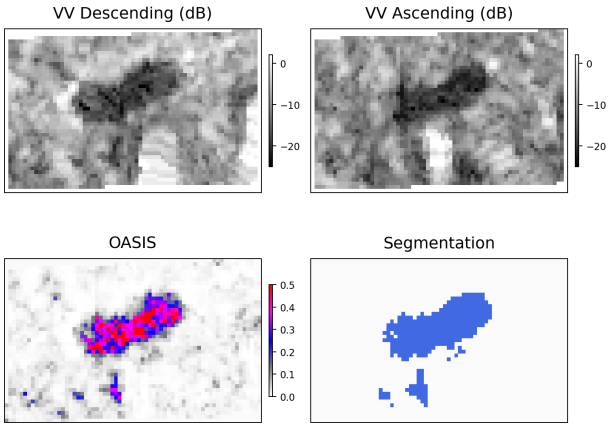

Figure 4. (top) SAR backscatter in VV polarisation from the descending orbit D139 on July 5, 2022 (left), and the ascending orbit A161 on July 6, 2022 (right). (bottom) The oasis index for 5–6 July 2022 (left) and its segmentation (right)

shown in the lower left panel of 4. We can observe that the oasis index shows stronger values at the Miage lake than around the lake, which makes its identification easier than by using individual backscattering maps. Once calculated, the oasis index is subsequently segmented to identify the lake's contours and estimate its area. For this task, we use a discrete-time dynamical system governed by various parameters similar to the system tested for the detection of wet snow from Sentinel-1 SAR images in (James et al., 2024). The dynamical system uses the oasis index as an initial condition and iteratively evolves it into a segmented image via bistable dynamics. The evolution law is essentially the same as in (James et al., 2024), although there are differences in the coupling rules between pixels. The lower right panel of Fig. 4 presents the segmentation results utilizing the oasis index for 5–6 July 2022.

4. Results and discussion

The automated optical observation workflow, based on the dual-threshold NDWI approach, was evaluated against reference data manually segmented on Sentinel-2 images for the 2022–2024 period (see Fig. 5), demonstrating high reliability in capturing the rapid surface area fluctuations of the Miage Lake.

The year 2022 provided a particularly significant dataset to test the algorithm's sensitivity during a major drainage event. Between June and August, the lake transitioned from a maximum extent of approximately 28000 m^2 to a nearly dry state. Both the HT (R^2 = 0.97) and ST (R^2 = 0.99) models exhibited excellent correlation with the reference data digitized from Sentinel-2 imagery, effectively tracking the shoreline recession. However, the HT showed a consistent negative bias of -1381 m^2, indicating that a conservative threshold fails to detect the shallow, saturated margins of the lake, leading to a systematic underestimation of the total water extent.

In contrast, the 2023 season was characterized by a dry summer for the Miage basin, during which the lake remained largely empty. This period served as a critical control for the algorithm's robustness against false positives; the HT matched the manually segmented reference data perfectly (0 m^2 detected), while the ST model exhibited only minor background noise (MAE = 300 m^2). This noise is likely attributable to damp debris or small ephemeral supraglacial ponds that were not recorded as permanent water bodies in the reference dataset but were spectrally close to the water threshold.

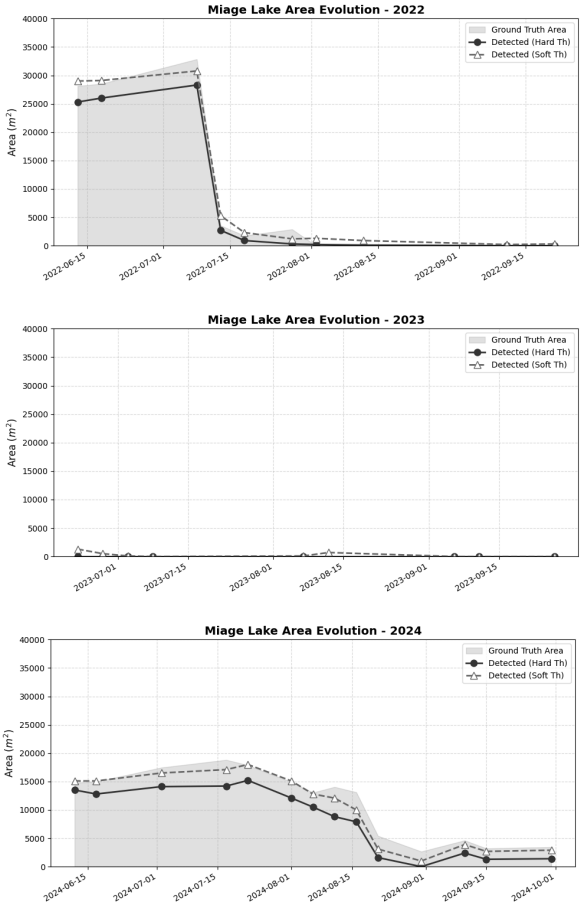

Figure 5. Multi-year time series comparison of the Miage Lake surface area for the summer seasons of 2022, 2023, and 2024. The plots illustrate the performance of the automated detection procedure using the HT (continuous line) and the ST (dashed line) procedure, compared to the reference area, manually digitized on Sentinel-2 imagery (shaded grey area).

The results from 2024 highlighted the impact of lake morphology on detection accuracy. During this season, the Miage Lake fragmented into due smaller, disconnected basins separated by debris ridges due to a lower water level. This fragmentation increased the total perimeter and the impact of mixed pixels at the debris-water interface, causing the HT model's performance to decrease (R^2 = 0.68) with a high negative bias. While the ST model proved more resilient (R^2 = 0.94) by capturing these transitional boundary pixels, the increased complexity of the lake's shape clearly elevated spatial uncertainty. This morphological complexity reinforces the need for a multi-sensor approach to manage variables like water turbidity or cloud cover.

To support this multi-sensor framework, the Random Forest algorithm was tested for regional-scale identification, demonstrating strong performance on the validation dataset with an 83% detection rate for the entire inventory and exceeding 92% for lakes larger than 900 m^2. Over-detection remained minimal when focusing on patches exceeding 1000 m^2, which accounted for approximately 200 polygons over the 12,000 km^2 study area. Using Miage Lake as a case study, the summer product was significantly more accurate than the yearly product (Fig. 3), though the former was more prone to localized false positives on shadowed hillsides or glacier surfaces. While this ML ap-

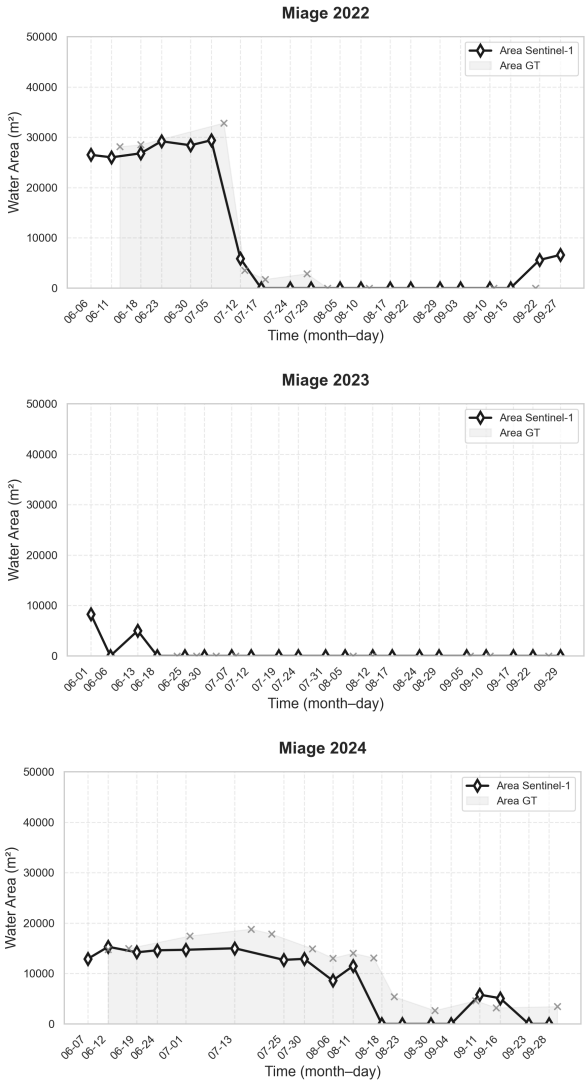

Figure 6. Multi-year time series comparison of the Miage Lake surface area for the summer seasons of 2022, 2023, and 2024. The plots illustrate the performance of the dynamical system segmentation method applied to oasis images, compared to the areas manually digitized on Sentinel-2 imagery (shaded gray area).

proach is highly effective for identifying and inventorying lake positions at a regional scale, it is currently unable to monitor area variations at a finer timescale than a season.

Consequently, the integration of radar data becomes essential to provide the high-frequency temporal resolution necessary to track morphological evolution regardless of weather conditions. The segmentation of the OASIS index obtained from SAR images yielded area estimates for the Miage Lake which were compared to the same manually segmented reference data derived from Sentinel-2 images (see Fig. 6). The comparison demonstrates a strong agreement between the radar-derived results and the optical reference database, aside from a minor underestimation of the areas by SAR. The SAR data accurately record the rapid phases of the lake's appearance and depletion. It should be noted that between 2022 and 2024, only Sentinel-1A was operational due to the loss of Sentinel-1B, resulting in a suboptimal configuration compared to dual-satellite observations. The successful launches of Sentinel-1C and Sentinel-1D will enable more frequent monitoring. However, the inherent time lag between Sentinel-1 and Sentinel-2 observation dates, combined with the rapid lake dynamics, remains a challenge when establishing an objective score between the radar estimates and the Sentinel-2 based reference data.

5. Conclusions

This study presented and validated an automated multi-sensor methodology for the continuous monitoring of glacial lakes in the Western Alps, with a specific focus on the highly dynamic Miage Lake. By integrating Sentinel-2 optical imagery with Sentinel-1 SAR data, we addressed several critical challenges inherent to high-mountain remote sensing, such as cloud cover and topographic noise. The results from the optical analysis demonstrate that a dual-threshold NDWI approach effectively captures complex lake dynamics, including the rapid drainage events observed in 2022. While the HT method provides a high-confidence core area essential for avoiding false positives in automated hazard systems, the ST algorithm is more capable of delineating the full lake extent, especially in cases of high water turbidity or lake fragmentation.

The 2024 monitoring season further highlighted that lake morphology—specifically the division of a single water body into multiple basins—significantly increases spatial uncertainty due to a higher perimeter-to-area ratio and the prevalence of mixed pixels. To manage these complexities, the research highlights a hierarchical monitoring strategy: ML algorithms are employed at a regional scale to identify and inventory lake positions, while the detailed tracking of morphological changes is achieved through targeted optical and radar analysis.

In particular, the integration of Sentinel-1 SAR data—utilizing the OASIS index coupled with iterative dynamical system-type algorithms—has proven essential to fill the temporal gaps left by optical sensors. This synergy provides a robust, all-weather monitoring capability that is crucial for real-time GLOF hazard and risk assessment. One of the promising avenues to pursue will be the complete fusion of optical and radar observations to achieve optimal monitoring of glacial lakes. In conclusion, the proposed workflow offers a scalable and robust solution for tracking the evolution of proglacial lakes in response to accelerating glacial retreat. Future research will focus on extending this methodology to a larger regional scale, aiming to integrate the optical, SAR, and machine learning components into a single, unified monitoring framework. This complete methodology will further enhance our capacity to monitor cryospheric transformations and mitigate associated risks across the broader alpine arc.

Acknowledgements

This work was carried out in the framework of the PNRR project "Agile Arvier. La cultura del cambiamento" – WP02 "Green Lab", CUP F87B22000380001. The authors acknowledge the financial support provided by the Direction Générale de la Prévention des Risques (DGPR) through the PAPROG (Action Plan for the Prevention of Glacial and Periglacial Risks) initiative. The authors acknowledge the European Space Agency and the Copernicus programme for providing Sentinel-1 SAR data and Sentinel-2 MS data.

References

Bolch, T., Buchroithner, M. F., Peters, J., Baessler, M., Bajracharya, S., 2008. Identification of glacier motion and potentially dangerous glacial lakes in the Mt. Everest region/Nepal using spaceborne imagery. *Natural Hazards and Earth System Sciences*, 8(6), 1329–1340.

Breiman, L., 2001. Random forests. *Machine learning*, 45(1), 5–32.

Costa, J. E., Schuster, R. L., 1988. The formation and failure of natural dams. *Geological society of America bulletin*, 100(7), 1054–1068.

Emmer, A., Allen, S. K., Carey, M., Frey, H., Huggel, C., Korup, O., Mergili, M., Sattar, A., Veh, G., Chen, T. Y. et al., 2022. Progress and challenges in glacial lake outburst flood research (2017–2021): a research community perspective. *Natural Hazards and Earth System Sciences Discussions*, 2022, 1–34.

Huggel, C., Kääb, A., Haeberli, W., Teysseire, P., Paul, F., 2002. Remote sensing based assessment of hazards from glacier lake outbursts: a case study in the Swiss Alps. *Canadian Geotechnical Journal*, 39(2), 316–330.

Huss, M., Bookhagen, B., Huggel, C., Jacobsen, D., Bradley, R. S., Clague, J. J., Vuille, M., Buytaert, W., Cayan, D. R., Greenwood, G. et al., 2017. Toward mountains without permanent snow and ice. *Earth's Future*, 5(5), 418–435.

James, G., Karbou, F., Durand, P., 2024. Dynamical System Approach for Wet Snow Retrieval in Mountains Using Sentinel-1 SAR Images. *IEEE Transactions on Geoscience and Remote Sensing*, 62, 1–10.

Karbou, F., James, G., Mauss, A., Verry, P., B. Demolis, R., Martin, 2026. Unlocking lakes in all terrain with Sentinel-1 SAR imagery.

Koleck, T., Hermitte, L., 2020. S1tiling, sentinel-1 preprocessing.

Kääb, A., Huggel, C., Fischer, L., Guex, S., Paul, F., Gärtner-Roer, I., Salzmann, N., Schlaefli, S., Schmutz, K., Schneider, D., Strozzi, T., Weidmann, Y., 2005. Remote sensing of glacier- and permafrost-related hazards in high mountains: An overview. *Natural Hazards and Earth System Sciences*, 5.

Miles, K. E., Willis, I. C., Benedek, C. L., Williamson, A. G., Tedesco, M., 2017. Toward monitoring surface and subsurface lakes on the Greenland ice sheet using Sentinel-1 SAR and Landsat-8 OLI imagery. *Frontiers in Earth Science*, 5, 251152.

Nagai, H., Ukita, J., Narama, C., Fujita, K., Sakai, A., Tadono, T., Yamanokuchi, T., Tomiyama, N., 2017. Evaluating the scale and potential of GLOF in the Bhutan Himalayas using a satellite-based integral glacier–glacial lake inventory. *Geosciences*, 7(3), 77.

Shugar, D., Burr, A., Haritashya, U., Kargel, J., Watson, C. S., Kennedy, M., Bevington, A., Betts, R., Harrison, S., Strattman, K., 2020. Rapid worldwide growth of glacial lakes since 1990. *Nature Climate Change*, 10, 939-945.

Taylor, C., Robinson, T., Dunning, S., Carr, J., Westoby, M., 2023. Glacial lake outburst floods threaten millions globally. *Nature Communications*, 14.

Troilo, F., Lodigiani, M., Nicora, M., Mondardini, L., Perret, P., Christille, J. M., Calabrese, M., Salvemini, C. B., Sartor, S., 2025. Monitoring cryospheric environment at a regional scale: Big data from sensor networks and experimental ai applications in the framework of the glarisk-cc fesr project. *New frontiers in Big Data and Artificial Intelligence (BDAI 2025)*.

Veh, G., Wang, B., Zirzow, A., Schmidt, C., Lützow, N., Steppat, F., Zhang, G., Vogel, K., Geertsema, M., Clague, J., Korup, O., 2025. Progressively smaller glacier lake outburst floods despite worldwide growth in lake area. *Nature Water*, 3.

Wangchuk, S., Bolch, T., Zawadzki, J., 2019. Towards automated mapping and monitoring of potentially dangerous glacial lakes in Bhutan Himalaya using Sentinel-1 Synthetic Aperture Radar data. *International journal of remote sensing*, 40(12), 4642–4667.

Zemp, M., Huss, M., Thibert, E., Eckert, N., McNabb, R., Huber, J., Barandun, M., Machguth, H., Nussbaumer, S. U., Gärtner-Roer, I. et al., 2019. Global glacier mass changes and their contributions to sea-level rise from 1961 to 2016. *Nature*, 568(7752), 382–386.

Zemp, M., Jakob, L., Dussaillant, I., Nussbaumer, S., Gourmelen, N., Dubber, S., Aa, G., Abdullahi, S., Andreassen, L. M., Berthier, E., Bhattacharya, A., Blazquez, A., Vock, L., Bolch, T., Box, J., Braun, M., Brun, F., Cicero, E., Colgan, W., Zheng, W., 2025. Community estimate of global glacier mass changes from 2000 to 2023. *Nature*, 639.

Zhang, G., Carrivick, J., Emmer, A., Shugar, D., Veh, G., Wang, X., Labedz, C., Mergili, M., Mölg, N., Huss, M., Allen, S., Sugiyama, S., Lützow, N., 2024. Characteristics and changes of glacial lakes and outburst floods. *Nature Reviews Earth Environment*.

Zheng, G., Bao, A., Allen, S., Ballesteros-Cánovas, J. A., Yuan, Y., Jiapaer, G., Stoffel, M., 2021. Numerous unreported glacial lake outburst floods in the Third Pole revealed by high-resolution satellite data and geomorphological evidence. *Sci. Bull*, 66, 1270–1273.